

N-linked Glycosylation Is Required for Optimal Function of Kaposi's Sarcoma Herpesvirus-encoded, but Not Cellular, Interleukin 6

Charles S. Dela Cruz,¹ Yoomi Lee,¹ Srinivas R. Viswanathan,¹
Ayman S. El-Guindy,¹ Jennifer Gerlach,⁴ Sarah Nikiforow,⁵
Duane Shedd,² Lyn Gradoville,² and George Miller^{1,2,3}

¹Department of Molecular Biophysics and Biochemistry, ²Department of Pediatrics, ³Department of Epidemiology and Public Health, ⁴Department of Microbiology, and ⁵Department of Immunobiology, Yale School of Medicine, New Haven, CT 06520

Abstract

Kaposi's sarcoma-associated herpesvirus interleukin-6 (vIL-6) is a structural and functional homologue of the human cytokine IL-6 (hIL-6). hIL-6 and vIL-6 exhibit similar biological functions and both act via the gp130 receptor subunit to activate the Janus tyrosine kinase (JAK)1 and signal transducer and activator of transcription (STAT)1/3 pathway. Here we show that vIL-6 is N-linked glycosylated at N78 and N89 and demonstrate that N-linked glycosylation at site N89 of vIL-6 markedly enhances binding to gp130, signaling through the JAK1-STAT1/3 pathway and functions in a cytokine-dependent cell proliferation bioassay. Although hIL-6 is also N-glycosylated at N73 and multiply O-glycosylated, neither N-linked nor O-linked glycosylation is necessary for IL-6 receptor α -dependent binding to gp130 or signaling through JAK1-STAT1/3. As distinct from vIL-6, unglycosylated hIL-6 is as potent as glycosylated hIL-6 in stimulating B cell proliferation. These findings highlight distinct functional roles of N-linked glycosylation in viral and cellular IL-6.

Key words: IL-6 • viral proteins • glycosylation • KSHV • cytokine

Introduction

Kaposi's sarcoma-associated herpesvirus (KSHV), herpesvirus 8, is a γ herpesvirus etiologically associated with Kaposi's sarcoma, multicentric Castleman's disease, and primary effusion lymphomas (PELs). Viral IL-6 (vIL-6), a structural and functional homologue of human IL-6 (hIL-6), is one of several homologues of cellular chemokines and cytokines encoded by KSHV (1). Although vIL-6 exhibits only 24.8% amino acid identity and 62.2% amino acid similarity with hIL-6 (2), it mimics a number of hIL-6 activities such as stimulating IL-6-dependent B cell line growth (3) and activating the Janus tyrosine kinase (JAK)1 and signal transducer and activator of transcription (STAT)1/3 pathway in HepG2 cells (4). hIL-6 is expressed by a number of cell types including B and T lymphocytes, monocytes, fibroblasts, keratinocytes, bone marrow stromal cells, endothelial cells, and astrocytes. The wide range of biological activities

attributed to hIL-6 includes the proliferation of lymphocytes and stem cells, differentiation of B cells and osteoclasts, induction of acute phase proteins in hepatocytes, and promotion of neuronal regeneration (5). hIL-6 serves as a growth factor for multiple myeloma and plasmacytoma cells (6). vIL-6 is expressed in KSHV-infected B cells and endothelial cells and induces proliferation, angiogenesis, and hematopoiesis in IL-6-dependent cell lineages (2, 7). vIL-6 can serve as an autocrine growth factor for PEL cell lines (8). Expression of vIL-6 accelerates hematopoiesis in mice and induces vascular endothelial growth factor, a factor implicated in PEL and Kaposi's sarcoma pathogenesis (9). However, the precise function of vIL-6 in KSHV pathogenesis is not well understood. vIL-6 may act as an antiapoptotic factor for survival of KSHV-infected cells and/or promote the proliferation of KSHV-infected cells or potential host cells.

The online version of this article contains supplemental material.

Address correspondence to George Miller, Department of Pediatrics, Yale University School of Medicine, Room 420 LSOB, 333 Cedar Street, New Haven, CT 06520. Phone: (203) 785-4758; Fax: (203) 785-6961; email: George.Miller@Yale.edu

Abbreviations used in this paper: hIL-6, human IL-6; HRP, horseradish peroxidase; JAK, Janus tyrosine kinase; KSHV, Kaposi's sarcoma-associated herpesvirus; PEL, primary effusion lymphoma; STAT, signal transducer and activator of transcription; TM, tunicamycin; vIL-6, viral IL-6.

Despite similarities in their global structures, hIL-6 and vIL-6 differ in their mode of receptor usage (10–12). vIL-6 and hIL-6 share with other cytokines, such as ciliary neurotrophic factor, leukemia inhibitory factor, oncostatin M, cardiotropin-1, and IL-11, the use of a gp130 receptor for signal transduction (13). Although both cellular IL-6 and vIL-6 bind gp130, the common signal transducing receptor subunit for the IL-6-type family of cytokines, hIL-6 requires a coreceptor, IL-6R α , for the assembly of a 2:2:2 hexameric signaling complex. Cytokines such as ciliary neurotrophic factor, leukemia inhibitory factor, oncostatin M, and IL-11 also require a specific coreceptor (13). In contrast, vIL-6 directly binds gp130 and does not require IL-6R α for signal transduction (7, 12). Cytokine binding to gp130 causes JAKs to phosphorylate STATs, which dimerize and translocate to the nucleus, where they bind specific enhancer sequences to stimulate or repress transcription of target genes. IFN- α produced in response to KSHV infection specifically down-regulates IL-6R α , making it difficult for hIL-6 to interact with its gp130 receptor (14). Because vIL-6 binds directly to the signaling gp130 receptor without first binding to IL-6R α , vIL-6 can exert its proliferative effects on B cells without being affected by IFN- α .

This study explores the hypothesis that differences in biological activity and receptor usage of cellular IL-6 and vIL-6 could be explained by differences in glycosylation of the two cytokines. Many cytokines are posttranslationally modified by the addition of sugar groups, which have the capacity to affect their biological function in a number of ways such as protein stability, protein secretion, receptor interaction, and subsequent downstream biological activity (15). Here we demonstrate that vIL-6 is glycosylated at two residues, N78 and N89. N-linked glycosylation of one of these residues, N89, is required for optimal gp130 receptor binding, JAK/STAT signaling, and stimulation of B cell proliferation. hIL-6 is known to be O- and N-linked glycosylated (16), but the functional role of the modification was unknown. We find that hIL-6 is N-glycosylated at one residue, N73, and O-glycosylated at T166 and T170/T171, but these glycosylations do not affect binding to the signaling receptor gp130, JAK/STAT activation, or B cell proliferation. These novel results show that a virally encoded cytokine such as IL-6 distinguishes itself from its cellular homologue through the functional importance of N-linked sugars.

Materials and Methods

Cell Culture and Transfections. HKB5/B5 is a hybrid cell line (provided by M.-S. Cho, Bayer Corp., Berkeley, CA) from fusion of Burkitt lymphoma-derived HH514-16 cells with 293 human embryonic kidney cell line. HKB5/B5 was used for transient transfections to produce mammalian-derived cellular IL-6 and vIL-6. Cells were grown in RPMI 1640 medium supplemented with 5% FCS at 37°C in 5% CO₂. Optimal transfection conditions of HKB5/B5 cells were achieved using the DMR1E-C reagent (Invitrogen; reference 17). To produce N-linked unglycosylated forms of vIL-6 and hIL-6, 0.2 or 1.0 μ g/ml tunicamycin

(TM) was added to the growth media. To produce O-linked unglycosylated forms of hIL-6, 1.0 μ g/ml monensin was used. Culture supernatants and cell extracts were prepared 48 h after transfection. B9.11, an IL-6-dependent mouse plasmacytoma cell line (18), and DS-1, an IL-6-dependent human B cell line (19), were used to measure IL-6 activity. These cells were maintained in RPMI 1640 medium supplemented with 5% FCS and 1 ng/ml hIL-6 (R&D Systems).

Plasmid Constructions. vIL-6 encoded in KSHV ORF K2 was generated by PCR from genomic cellular DNA preparations of PEL cell lines BC1, BC-3, and HHB2 (20). The PCR products contained flanking AseI and XhoI sites. Purified PCR products were cloned into the prokaryotic expression vector pET22 (Novagen) using the restriction sites NdeI and XhoI. vIL-6 PCR products were also cloned into the eukaryotic vector pcDNA3.1 (Invitrogen) using the BamHI and XhoI sites. hIL-6 cDNA was cloned into the EcoRI site of the pcDNA3.1 plasmid vector. Glycosylation site mutants of vIL-6 and hIL-6 were generated using a QuikChange site-directed mutagenesis kit (Stratagene). The vIL-6 and hIL-6 genes in all clones were sequenced in their entirety.

Bacterial Expression of vIL-6. Each clone was transformed into BL21(DE3) cells. In all purifications, fresh transformants were grown overnight, culture was incubated at 37°C until the OD 600 was 0.6–0.7, and cells were induced for 2 h using 1 mM IPTG. Cells were pelleted, resuspended in 40 ml buffer A (5 mM imidazole, 500 mM NaCl, 20 mM Tris, pH 7.9), sonicated three times for 15 s, and centrifuged in a SW28 rotor at 20 K for 15 min. The pellet was resuspended in buffer A with 6 M urea, sonicated twice, and placed on ice for 1 h. The supernatant was loaded on a Ni⁺⁺ agarose column (QIAGEN). The column was washed with buffer A and buffer B (60 mM imidazole, 500 mM NaCl, 20 mM Tris, pH 7.9). The protein was eluted from the column with a step gradient of 0.1–1 M imidazole in 1-ml fractions. The fractions were dialyzed in RPMI medium for 2 h, aliquoted, and stored at –80°C. The purified bacterial vIL-6 protein samples were then analyzed by Western blot using an anti-KSHV IL-6 polyclonal rabbit antisera. The Immunization Service of the Yale Animal Resources Center hyperimmunized rabbits with the KSHV IL-6 peptide (PDVTPDVHDK) conjugated to KLH.

Western Blot Analysis. Extracts were prepared from transfected HKB5/B5 cells grown in culture for 48 h. A total of 2 \times 10⁶ cells were resuspended in 100 μ l SDS sample buffer and sonicated for 15 s. Samples were boiled for 5 min and electrophoresed through a 10% polyacrylamide gel. Cell extracts loaded in the Western blots consisted of \sim 0.5 \times 10⁶ transfected HKB5/B5 or HepG2 cells. For vIL-6 or hIL-6 protein in HKB5/B5 transfectant supernatants, \sim 10 ng protein was loaded. A 1:200 dilution of vIL-6 rabbit polyclonal antiserum for vIL-6 protein or 1 μ g/ml hIL-6 goat polyclonal antibody (R&D Systems) followed by a 1:200 dilution of a rabbit anti-goat Ig bridge (Sigma-Aldrich) was used for vIL-6 or hIL-6 protein detection, respectively. Immunoreactive bands were detected with ¹²⁵I-labeled protein A and autoradiography. For the detection of STAT1 protein and its phosphorylated form, antibodies sc-417 and sc-8394, respectively, were used (Santa Cruz Biotechnology, Inc.).

ELISA for vIL-6 or hIL-6. To detect vIL-6 by ELISA, wells were coated with 2 μ g/ml protein A agarose-purified Ig fraction of rabbit antiserum to vIL-6 diluted in 100 μ l coating buffer (0.1 M carbonate, pH 9.5). Plates were incubated at 4°C overnight. The wells were washed three times with PBS containing 0.05% (vol/vol) Tween and blocked with 10% FCS in PBS for 3 h at room temperature. After additional washes, serially diluted cul-

ture supernatants were added. Purified *Escherichia coli*-derived vIL-6 was used for generating a standard curve. Samples were incubated overnight at 4°C. After further washes, 100 µl biotinylated anti-KSHV IL-6 rabbit antiserum at 2 µg/ml was added for 1 h at room temperature. After PBS/Tween washes, streptavidin conjugated to horseradish peroxidase (HRP; Zymed Laboratories) at a dilution of 1:3,000 in FCS blocking buffer for 30 min was added. After 10 washes in PBS/Tween, peroxidase activity was detected by adding 50 µl/well tetramethylbenzidine substrate reagent (BD Biosciences). Reaction was stopped using 50 µl 2N H₂SO₄. Absorbances were read at 450 nm using a Coulter MR5000 ELISA reader (Dynatech). To detect hIL-6, 2 µg/ml polyclonal anti-hIL-6 goat antibody (R&D Systems) was used as the capturing antibody and 0.5 µg/ml monoclonal anti-hIL-6 mouse antibody was used as the detecting antibody (R&D Systems) followed by the secondary antibody donkey anti-mouse IgG HRP (Jackson ImmunoResearch Laboratories). Recombinant hIL-6 (R&D Systems) was used as standard.

ELISA for Binding of IL-6 to gp130. ELISA plates were coated with soluble gp130 (R&D Systems) at 625 ng/ml in carbonate buffer overnight. After washing with PBS/Tween and blocking with PBS/10% FCS for 3 h, wells were loaded with the vIL-6 supernatants and incubated at 4°C. After washing, vIL-6 that bound to the sgp130 was detected using 100 µl biotinylated anti-KSHV IL-6 rabbit antiserum at 2 µg/ml and the secondary reagent of streptavidin conjugated to HRP. For hIL-6, ELISA plates previously coated with sgp130 were washed and blocked with PBS/10% FCS before the addition of hIL-6 supernatants mixed with 625 ng/ml sIL6-Rα (R&D Systems). After overnight incubation at 4°C and multiple washings, bound hIL-6 was detected with 2 µg/ml polyclonal anti-hIL-6 goat antibody and donkey anti-goat IgG HRP followed by chromogenic substrates.

B9.11 and DS-1 Cell Proliferation Assays. B9.11 or DS-1 cells were washed three times in RPMI 1640 medium without IL-6. Cells were plated at 4 × 10⁴ cells per 100-µl well in the presence or absence of vIL-6 and hIL-6 preparations. Recombinant bacterial vIL-6 was purified as described above. Purified recombinant bacterial hIL-6 was purchased from R&D Systems. Recombinant forms of both cytokines were expressed in HKB5/B5 cells. After 2 (B9.11) or 4 d (DS-1) of culturing in the presence of serially diluted IL-6 samples, cells were pulsed with 1 µl (³H) tritiated thymidine for 12–16 h. Proliferation of cells was determined by thymidine incorporation using a 96-well cell harvester and a β-scintillation counter. B cell proliferative responses were expressed as mean [³H]thymidine incorporation (cpm) ± standard errors of triplicate cultures.

Luciferase Assay. Transient transfections were performed in HepG2 cells using transfection reagent DMRIE-C. Cells were seeded in six-well plates at 1–2 × 10⁶ cells/well in RPMI 1640 containing 10% FCS 24 h before transfection. After culture supernatants were removed, the adherent HepG2 cells were transfected with DMRIE-C reagent premixed with the reporter plasmids pGAS/Luc or pLuc in OPTI-MEM medium (Invitrogen) for 4 h. Cells were incubated for 48 h before treatment with vIL-6 and hIL-6 preparations for another 6 h. Cell lysates were prepared by extraction with 200 µl lysis buffer from the Luciferase Reporter Gene Assay (Roche) and luciferase activities were measured using a Lumat luminometer (LB9501; Roche) for 10 s.

Online Supplemental Material. Fig. S1 demonstrates that unglycosylated hIL-6 expressed in *E. coli*, unglycosylated hIL-6 produced in mammalian cells (through quadruple mutagenesis and use of glycosylation inhibitors), and fully glycosylated hIL-6 proteins have similar biological potency in stimulating B9.11 cell

proliferation. Fig. S1 is available at <http://www.jem.org/cgi/content/full/jem.20031205/DC1>.

Results

Differences in KSHV IL-6 Expressed in *E. coli* and Mammalian Cells. To study the function of KSHV IL-6, the protein was prepared from both bacterial and mammalian sources. vIL-6 was cloned with a six-residue histidine tag into the pET-22 vector and purified from *E. coli* using a nickel column. vIL-6 was also cloned into the mammalian vector pcDNA3.1 and expressed in human HKB5/B5 cells. Western blot analysis using polyclonal rabbit antiserum to vIL-6 revealed differences in electrophoretic mobility of vIL-6 depending on the source of the protein. There were three major immunoreactive protein products present in extracts of HKB5/B5 cells transfected with vIL-6 (Fig. 1 A, lane 2). The largest and most abundant of these products,

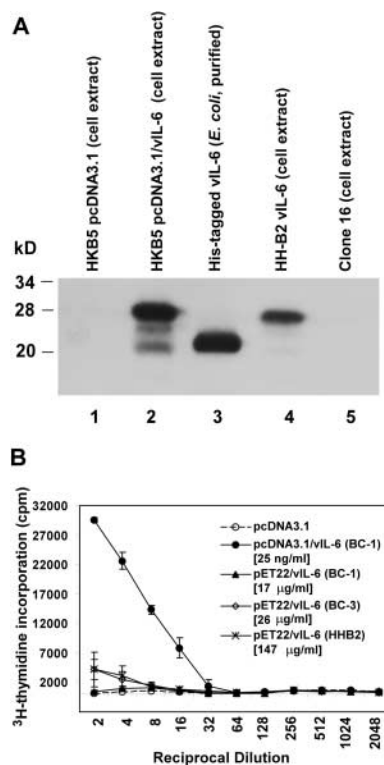


Figure 1. Comparison of vIL-6 expressed in *E. coli* and in eukaryotic cells. (A) Comparison of electrophoretic mobility of vIL-6 from various sources. An immunoblot reacted with polyclonal rabbit antibody to vIL-6. Lane 1, extract of HKB5 cells transfected with pcDNA3.1; lane 2, extract of HKB5/B5 cells transfected with pcDNA3.1/vIL-6; lane 3, purified vIL-6 expressed in *E. coli*; lane 4, extracts of HHB2 cells, a KSHV⁺ PEL cell line; lane 5, extract of HH514-16 (clone16), an EBV⁺ KSHV⁻ Burkitt lymphoma cell line. (B) Comparison of biological activity of vIL-6-expressed mammalian cells or *E. coli* in a B9.11 cell proliferation assay. B9.11 cells were incubated with supernatants of HKB5/B5 cells transfected with pcDNA3.1 or pcDNA3.1/vIL-6 (BC-1). B9.11 cells were also incubated with vIL-6 from three KSHV strains cloned in pET22, expressed in *E. coli*, and purified on Ni²⁺ columns. The concentration of vIL-6 expressed in eukaryotic cells was 25 ng/ml. The concentration of vIL-6 expressed in *E. coli* varied from 17 to 147 µg/ml.

~28 kD, comigrated with vIL-6 expressed during the KSHV lytic cycle in HHB2 cells, a KSHV-infected PEL cell line (Fig. 1 A, lane 4). An EBV-infected Burkitt lymphoma cell line contained no immunoreactive vIL-6 (Fig. 1 A, lane 5). *E. coli*-produced His-tagged vIL-6 protein (Fig. 1 A, lane 3) showed one predominant polypeptide, ~21 kD, which was slightly larger in molecular weight than the smallest form of vIL-6 present in human cells (Fig. 1 A, lane 2). We postulated that the electrophoretic mobility of the *E. coli*-expressed vIL-6 could be accounted for by an unmodified form of the protein containing additional residues from the histidine tags.

KSHV IL-6 proteins derived from *E. coli* or mammalian cells were tested for their ability to stimulate the proliferation of IL-6-dependent B9.11 cell line using a thymidine incorporation assay. vIL-6 secreted from the HKB5/B5 mammalian cell line potently activated B9.11 cell proliferation (Fig. 1 B). Purified vIL-6 proteins derived from three different KSHV strains expressed in *E. coli* only minimally stimulated the B9.11 cells, even though vIL-6 purified from *E. coli* contained >1,000-fold more protein. The addition of vIL-6 made in human cells to vIL-6 produced in bacteria restored maximum proliferation of B9.11 cells, indicating that poor response to bacterial-derived vIL-6 was not due to toxicity (unpublished data). These findings suggested that posttranslational modifications of vIL-6 that occurred in human cells, but not in *E. coli*, might be important for its biological function.

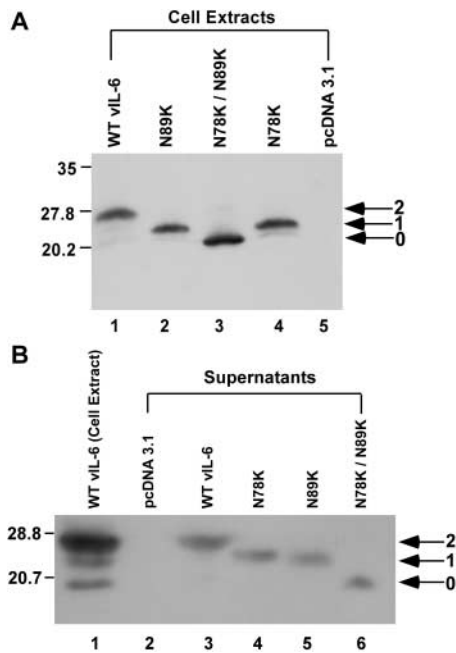


Figure 2. Comparison of electrophoretic mobility of wild-type and N-linked glycosylation site mutants of vIL-6. Wild-type vIL-6 and N-linked glycosylation site mutants (N78K, N89K, and N78K/N89K) were expressed in HKB5/B5 cells. Immunoblots were probed with polyclonal antibodies to vIL-6. (A) Cell extracts. (B) Culture supernatants concentrated ~13-fold by dialysis against polyethylene glycol. Arrows indicate doubly, singly, and unglycosylated forms of the protein.

N-linked Glycosylation Site Mutants of KSHV IL-6. The vIL-6 protein has two potential N-linked glycosylation consensus sites, as represented by Asn-X-Ser/Thr, where X can be any amino acid. These are located at N78 and N89. The three forms of vIL-6 observed in HKB5/B5 cells (Fig. 1 A, lane 2) could be explained by forms of the protein with both sites, one site, or no sites glycosylated. To explore this possibility, site-directed mutants, N78K and N89K, and the double mutant N78K/N89K, were generated. These mutations retain a functional amine group but cannot be glycosylated. The electrophoretic mobility of the mutants was compared with wild-type vIL-6 in cell extracts and supernatants of transfected HKB5/B5 cells (Fig. 2). Wild-type vIL-6 migrated more slowly, at 28 kD, than either single N-linked glycosylation site mutant, which migrated at ~25 kD. The double mutant that lacked both N-linked glycosylation sites migrated fastest at ~22 kD. These findings were most consistent with N-linked glycosylation of both residues in the wild-type protein. All the mutant vIL-6 proteins were produced in amounts approximately equal to wild-type and were secreted in equal amounts (see Fig. 5 C).

Effect of TM on Electrophoretic Mobility of KSHV IL-6 Protein. To confirm that the differences in electrophoretic mobility of wild-type vIL-6 and mutant forms of vIL-6 were the result of N-linked glycosylation, the proteins were expressed in HKB5/B5 cells treated with TM (Fig. 3). When wild-type vIL-6 was produced in the presence of TM, the mobility of the vIL-6 polypeptide shifted from a predominantly 28-kD form (Fig. 3, lane 2) to a 22-kD form (Fig. 3, lanes 3 and 4), which comigrated with the N78K/N89K double mutant (Fig. 3, lane 5). TM treatment of cells expressing the single glycosylation site mutants, N78K and N89K, resulted in a change in electro-

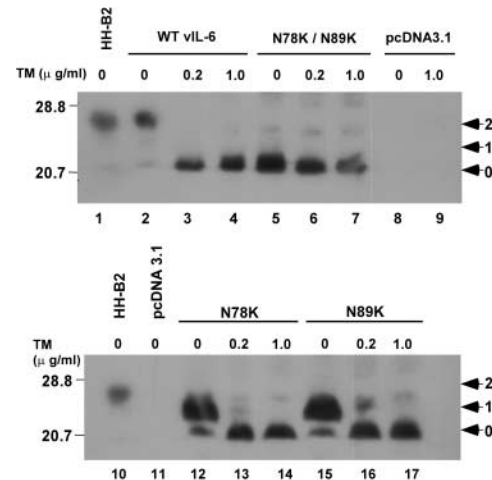


Figure 3. Effect of TM on electrophoretic mobility of vIL-6. HKB5/B5 cells were transfected with wild-type or N-linked glycosylation site mutants of vIL-6. The cells were untreated (lanes 2, 5, 8, 12, and 15) or received 0.2 (lanes 3, 6, 9, 13, and 16) or 1.0 μg/ml (lanes 4, 7, 11, 14, and 17) TM. Lanes 1 and 10, HH-B2 cell extracts; lanes 2-4, vIL-6; lanes 5-7, N78K/N89K; lanes 8, 9, and 11, pcDNA3; lanes 12-14, N78K; lanes 15-17, N89K.

phoretic mobility from a predominant 25-kD form to the 22-kD form. TM treatment did not affect the electrophoretic mobility of vIL-6 expressed by the mutant N78K/N89K (Fig. 3, lanes 5–7). These results showed that in wild-type vIL-6, both N78 and N89 were N-linked glycosylated. The predominant 28-kD protein represents the doubly N-linked glycosylated form of vIL-6, the 25-kD protein represents the two singly N-linked glycosylated species, and the 22-kD protein represents a non-N-linked glycosylated form of vIL-6 protein.

Requirement of N89 in KSHV IL-6 for Optimal Function in B9.11 Cytokine-dependent Cell Proliferation Assay. To determine whether specific N-linked glycosylation of vIL-6 was required for its biological function and could explain the nonoptimal function of nonglycosylated, bacterially produced vIL-6, supernatants from HKB5/B5 cells transfected with different vIL-6 N-linked glycosylation mutant constructs containing equal amounts of immunoreactive vIL-6 were assessed for their capacity to stimulate B9.11 cell growth. By comparison to wild-type vIL-6 and the N78K mutant, the N89K and N78K/N89K double mutants of vIL-6 were 16-fold impaired in their ability to stimulate proliferation of B9.11 cells (Fig. 4). This result suggested that N-linked glycosylation at site N89 was important for vIL-6 function, whereas N78 site was not essential. Another interpretation of this result was that the N89K mutation created a form of vIL-6 that inhibited B9.11 cell proliferation. Experiments were performed in which N89K vIL-6 protein was combined with wild-type vIL-6 to determine whether N89K acted as a dominant negative mutant. An additive effect on B9.11 cell proliferation was observed when N89K vIL-6 supernatants were mixed with wild-type vIL-6 (unpublished data). Similarly, HKB5/B5 cells were cotransfected with N89K vIL-6 and wild-type vIL-6 plasmids to determine if N89K mutant vIL-6 could block wild-type vIL-6 intracellularly. Results of B9.11 cell proliferation assays using supernatants from the cotransfected cells showed no inhibition of

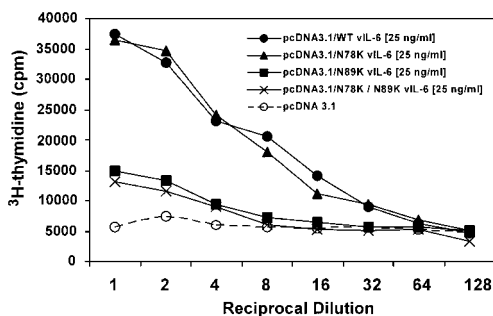


Figure 4. N89 of KSHV IL-6 is required for optimal function in a B9.11 cell cytokine-dependent proliferation assay. Two-fold serially diluted supernatants, containing 25 ng/ml vIL-6 protein as determined by vIL-6-specific ELISA, derived from HKB5/B5 cells transfected with plasmids encoding wild-type vIL-6, or mutants N78K, N89K, and N78K/N89K were assessed for their capacity to stimulate proliferation of B9.11 cells. Cells were pulsed with tritiated thymidine from 48 to 64 h after addition of the supernatants, and radioactivity incorporation (cpm) was determined.

wild-type vIL-6 activity by the mutant N89K form (unpublished data).

Site-directed mutants N78Q, N89Q, and N78Q/N89Q of vIL-6 were also produced in HKB5/B5 cells. vIL-6 encoded by these mutants were secreted in equal amounts, but the N89Q and double mutant forms were again 16-fold impaired in stimulating proliferation of B9.11 cells (unpublished data). Wild-type and N-linked glycosylation site mutants of vIL-6 were also tested on DS-1, a human B cell line that is cytokine dependent (19). In this assay, the N89K and N78K/N89K double mutant were impaired in their ability to stimulate DS-1 cells by comparison to wild-

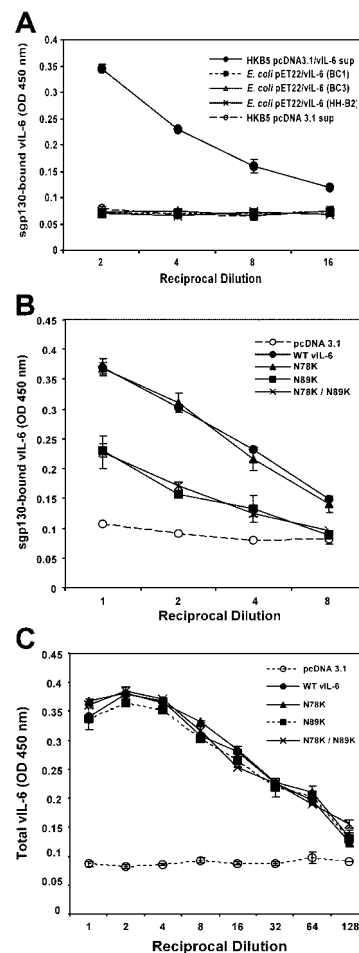


Figure 5. Comparison of binding to gp130 by wild-type and N-linked glycosylation site mutants of vIL-6. (A) Comparison of binding to sgp130 by vIL-6 expressed in HKB5/B5 cells and in *E. coli*. Soluble gp130 was coated on plastic plates. Serial dilutions starting at 20 ng/ml purified *E. coli*-derived wild-type vIL-6 from three different KSHV strains and HKB5/B5-derived wild-type vIL-6 were assessed for binding to gp130 by ELISA. (B) Comparison of binding to sgp130 by wild-type vIL-6 and N-linked glycosylation site mutants. Supernatants from transfected HKB5/B5 cells containing equal amounts of vIL-6 or its mutants were assessed for their capacity to bind to sgp130 by an ELISA. (C) Assay for the amount of immunoreactive vIL-6 added to sgp130 in the experiment shown in Fig. 5 B. Plates were coated with purified polyclonal rabbit anti-vIL-6 IgG. In experiments shown in A, B, and C, the amount of vIL-6 bound was detected with biotinylated polyclonal rabbit antibody to KSHV IL-6.

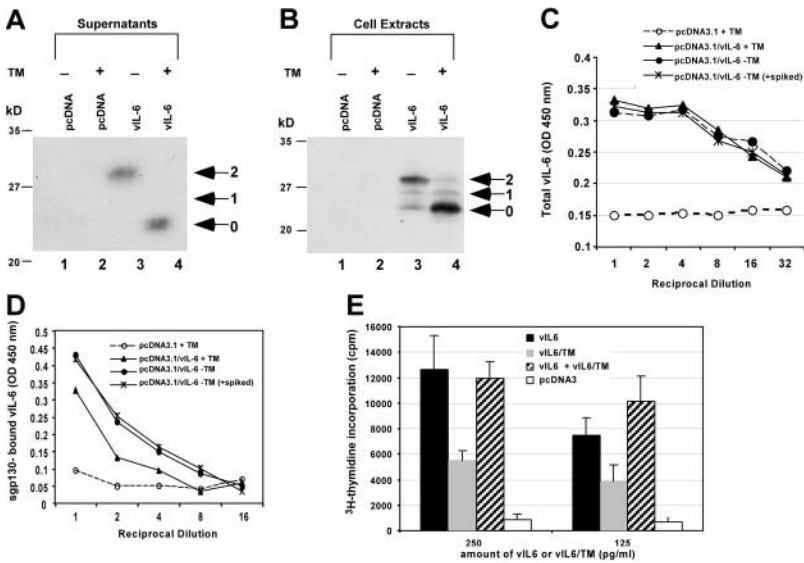


Figure 6. Effect of expression of vIL-6 in the presence of TM on binding to sgp130 and on B9.11 cell proliferation. (A and B) Electrophoretic mobility of vIL-6 expressed in HKB5/B5 cells in the absence or presence of 1.0 μ g/ml TM. Immunoblots of culture supernatants (A) or cell extracts (B) were reacted with polyclonal rabbit antibody to vIL-6. The preparation shown in A was used for experiments illustrated in panels C–E. (C) ELISA assay for the amount of vIL-6 present in supernatants of HKB5/B5 cells transfected with pcDNA3.1 or pcDNA3.1/vIL-6, treated or untreated with TM. (D) ELISA assay for binding of vIL-6 to sgp130. In one sample, vIL-6 expressed in the absence of TM was spiked with TM before assaying its binding to sgp130. (E) B9.11 assay of vIL-6 expressed in the absence of TM (solid bars), the presence of TM (shaded bars), or vIL-6 expressed in the presence of TM to which untreated vIL-6 was added (hatched bars).

type and N78K vIL-6 to a similar extent as they were in the B9.11 cell assay (unpublished data).

KSHV IL-6 N-linked Glycosylation Site Variants Are Impaired in Binding to sgp130. The human homologue of IL-6 must bind to the high affinity α subunit of IL-6R (IL-6R α) before it engages the signal-transducing β subunit gp130 (13). However, vIL-6 can directly bind and trigger the gp130 receptor independent of IL-6R α (21). Various forms of vIL-6 were studied for binding to sgp130 using an ELISA assay we developed (Fig. 5). Using equal amounts of immunoreactive vIL-6, the cytokine cloned from three different KSHV⁺ cells lines (BC1, BC3, and HH-B2) expressed in bacterial cells, which exhibited relatively poor proliferative ability to stimulate B9.11 cells (Fig. 1 B), was also impaired in its capacity to bind sgp130 when compared with its mammalian cell-derived counterpart (Fig. 5 A). Mutants N89K and N78K/N89K expressed in human cells were approximately threefold impaired in binding sgp130 in comparison to wild-type and N78K vIL-6 (Fig. 5 B). Wild-type vIL-6 and the mutants used in the binding assays contained equal amounts of immunoreactive vIL-6 (Fig. 5 C). These experiments provided a correlation between the ability of the mutants to bind the sgp130 receptor and the capacity to stimulate proliferation of cytokine-dependent B9.11 cells.

TM Inhibits Binding to sgp130 and Functional Activity of KSHV IL-6. To establish whether the impaired binding of the N89K and N78K/N89K mutants was due to alterations of glycosylation, we compared binding to sgp130 of wild-type vIL-6 expressed in the presence or absence of TM (Fig. 6). The effect of TM on the secreted vIL-6 preparation used for the experiments was to change it from a fully glycosylated to an unglycosylated form (Fig. 6, A and B). TM slightly reduced the amount of immunoreactive vIL-6 that was secreted, however, equal amounts of vIL-6 were used for the binding studies (Fig. 6 C). vIL-6 expressed in the presence of TM bound to sgp130 approximately two- to threefold less well than wild-type vIL-6

(Fig. 6 D). The extent of impairment in binding of vIL-6 expressed in the presence of TM (Fig. 6 D) was similar to the impairment in binding by the N89K and N78K/N89K mutants (Fig. 5 B). TM added in the binding assay to wild-type vIL-6 expressed in the absence of the inhibitor did not affect binding of vIL-6 to sgp130 (Fig. 6 D).

The decrease in binding to sgp130 of vIL-6 expressed in the presence of TM was reflected in a decrease in the capacity of vIL-6 to stimulate proliferation of B9.11 cells (Fig. 6 E). Culture supernatants of HKB5/B5 cells treated with TM were toxic to the B9.11 cells, however, this toxicity was eliminated by diluting the supernatant at 1:120. Therefore, we compared the biologic activity of vIL-6 and vIL-6/TM in concentrations of 250 and 125 pg/ml (Fig. 6 E). At these concentrations, vIL-6/TM was approximately two- to threefold less active than vIL-6 produced in the absence of TM. The addition of wild-type vIL-6 to vIL-6/TM restored wild-type activity, indicating that there was no residual toxicity in the TM-treated samples.

Diminished STAT Protein Activation by N-linked Glycosylation KSHV IL-6 Mutants. Cellular and KSHV IL-6 homologues exert their activity by inducing oligomer formation of gp130 transmembrane signaling protein (22). These oligomers recruit JAK proteins, which phosphorylate the STAT family of transcription factors leading to their translocation to the nucleus for gene activation. We studied the impact of the N-linked glycosylation site mutants on the JAK/STAT signaling pathway by means of a reporter assay in which luciferase expression is under the control of STAT1 binding to three oligomerized IFN- γ response elements (pGAS3/Luc; Fig. 7 A). HepG2 cells transfected with the pGAS3/Luc or pLuc reporters were treated with cell culture supernatants containing equal amounts of vIL-6 or the N-linked glycosylation site mutants for 6 h before luciferase activity was measured. KSHV IL-6 mutants defective in N-linked glycosylation at site N89 (N89K and N78K/N89K mutants) were approximately fourfold reduced in capacity to activate the

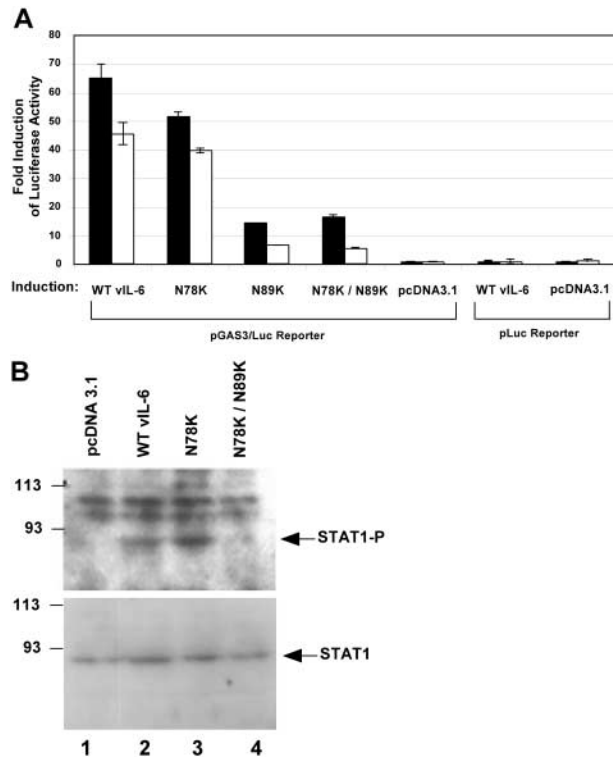


Figure 7. STAT signaling by wild-type vIL-6 and N-linked glycosylation site mutants. (A) HepG2 cells were transfected with pGAS3/Luc, a STAT1-responsive reporter, or pLuc control reporter. After 48 h, the cells were treated with 500 (solid bars) or 250 μ l (open bars) supernatants from HKB5/B5 cells transfected with wild-type vIL-6, N78K, N89K, N78K/N89K double mutant, or pcDNA3.1 vector. Luciferase activity was measured 6 h after the addition of supernatants. (B) Immunoblot of extracts of HepG2 cells treated with vIL-6, N78K, or N78K/N89K double mutant using antibodies to phosphorylated STAT1 (top) or STAT1 (bottom).

JAK/STAT signaling pathway compared with the activity of wild-type protein or of the N78K mutant (Fig. 7 A). Cell lysates of HepG2 cells treated with wild-type and the N78K mutant contained amounts of phosphorylated STAT1 protein readily detectable by immunoblotting (Fig. 7 B). However, the amount of phosphorylated STAT1 protein in the cell lysates of HepG2 cells treated with the N78K/N89K vIL-6 mutant was markedly reduced (Fig. 7 B). Comparable amounts of STAT1 protein were present in the cell extracts.

N-linked Glycosylation of hIL-6 Is Not Required for Activity. Human cellular IL-6 is known to be N-linked and O-linked glycosylated, but the functional importance of the N-linked glycosylation sites is not known. There are two N-linked glycosylation consensus sites at N73 and N172. Single (N73K and N172K) and double (N73K/N172K) mutants of hIL-6 proteins were generated by site-directed mutagenesis. The wild-type hIL-6 and mutant proteins produced in HKB5/B5 cells were analyzed on Western blots (Fig. 8). Unlike vIL-6 in which the large 28-kD form expressed in HKB5/B5 cells was predominant (Fig. 2 B), the predominant form of secreted hIL-6 was the broad 21-kD form. The electrophoretic mobility of N172K mutant

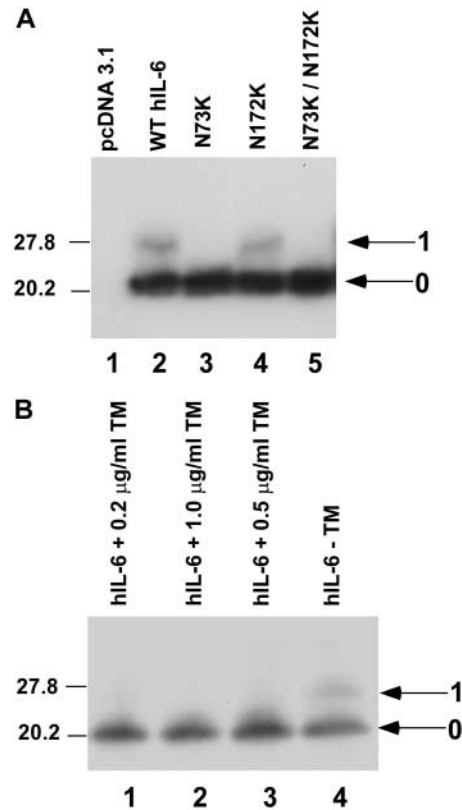


Figure 8. N-linked glycosylation of hIL-6. (A) Electrophoretic mobility of wild-type hIL-6 and two N-linked glycosylation site mutants of hIL-6 expressed in HKB5/B5 cells. (B) Effect of TM on electrophoretic mobility. HKB5/B5 cells were transfected with pcDNA3.1/hIL-6 in the presence of increasing concentrations of TM (lanes 1–3) or no TM (lane 4). Both immunoblots were reacted with polyclonal antibody to hIL-6.

was identical to wild-type. Mutants N73K and N73K/N172K expressed only the 21-kD form of the protein. Furthermore, expression of hIL-6 in the presence of TM (Fig. 8 B) eliminated the 27-kD form. These experiments indicated that hIL-6 contained a single functional N-linked glycosylation site at N73.

N-linked glycosylation did not affect the secretion of cellular IL-6 (Fig. 9 A). Wild-type hIL-6 and the N-linked glycosylation site mutants bound to sgp130 to a similar extent, only in the presence of soluble IL6-R α (Fig. 9 B). N-linked glycosylation site mutagenesis did not alter binding to sgp130. Furthermore, unlike vIL-6 in which the N89K mutant cytokine was impaired at stimulating cell proliferation, the N73K glycosylation site mutation in hIL-6 did not impair JAK/STAT signaling (Fig. 9 C), B9.11, or DS-1 cell proliferation (Fig. 9 D and unpublished data).

Neither N-linked nor O-linked Glycosylation of hIL-6 Is Required for Optimal Activity. The majority of hIL-6 molecules are O-glycosylated, whereas a minority are N-glycosylated (Fig. 10, A and B). Through mutagenesis, we found that O-glycosylation of hIL-6 occurs at sites T166, T170, and/or T171. A triple mutant of hIL-6 with T to A substitutions at each of these sites showed the absence of the \sim 22-kD band representing the O-glycosylated form of

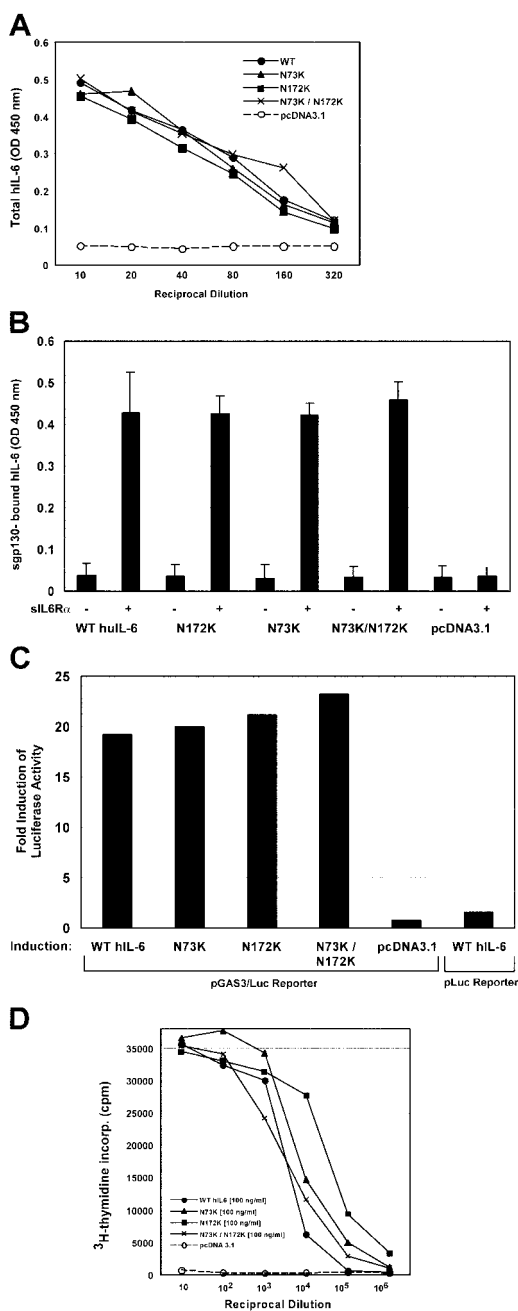


Figure 9. N-linked glycosylation is not required for hIL-6 receptor binding, STAT signaling or cytokine-dependent B9.11 cell proliferation. (A) Calibration of quantities of hIL-6 and N-linked glycosylation site mutants secreted from transfected HKB5/B5 cells. ELISA plates were coated with polyclonal goat antibody to hIL-6, and hIL-6 was quantitated with monoclonal mouse antibody to hIL-6 conjugated to HRP. All the hIL-6 supernatants contained 100 ng/ml hIL-6 protein. (B) Binding to sgp130 in the presence or absence of soluble IL-6R α . ELISA plates were coated with sgp130. Culture supernatants mixed with soluble IL-6R α , or untreated, were assessed for binding to sgp130 by ELISA. (C) Supernatants from HKB5/B5 cells transfected with wild-type hIL-6 or N-linked glycosylation site mutants were assessed for their capacity to activate a STAT1-responsive reporter, pGAS3/Luc. (D) B9.11 cell proliferation assay in response to wild-type and N-linked glycosylation site mutants of hIL-6.

hIL-6 and the presence of the \sim 20-kD unglycosylated form of the protein (Fig. 10, A and B). This triple mutant was maximally functionally active in stimulating the IL-6–dependent B9.11 cells as compared with the wild-type protein (Fig. 10 D). Moreover, a triple mutant of hIL-6 lacking the three O-glycosylation sites that additionally lacks the N73 glycan was found to lack all forms of glycosylation as shown in Fig. 10 A. This fully unglycosylated mutant form of hIL-6 was equally capable of binding to gp130/IL-6R α and stimulating proliferation of the B9.11 cells as the wild-type protein (Fig. 10, C and D). We also made hIL-6 in the presence of monensin, an inhibitor of O-glycosylation, and TM to produce hIL-6 lacking both O-glycans and N-glycans (Fig. 10 B, lanes 5 and 6). hIL-6 made in the presence of these inhibitors was as active as wild-type in binding gp130/IL-6R α and in stimulating B9.11 cell proliferation (Fig. 10, C and E). Thus, both N-linked and O-linked glycans on hIL-6 made in mammalian cells are dispensable for the functional assays we used. Moreover, the lack of importance of N-glycans in hIL-6 cannot be accounted for by the presence of O-glycans. Recombinant hIL-6 protein expressed in *E. coli* bacteria, which are not known to glycosylate protein, was equally active in stimulating B9.11 cell proliferation as comparable amounts of the fully glycosylated hIL-6 protein were made in mammalian cells (Fig. S1, available at <http://www.jem.org/cgi/content/full/jem.20031205/DC1>).

Glycosylated hIL-6 Is More Potent than Glycosylated KSHV IL-6. To compare the biological activity of cellular IL-6 and vIL-6 that were expressed in mammalian HKB5/B5 cells, we used equal amounts of the fully glycosylated wild-type hIL-6 and vIL-6 to stimulate B9.11 cell proliferation. The fully glycosylated form of hIL-6 was \sim 100 times more potent in stimulating the IL-6–dependent cell growth than the fully glycosylated form of vIL-6 (Fig. 11).

Discussion

Relative Importance of N-linked Glycosylation of vIL-6 and hIL-6. This report provides novel information about the relative importance of N-linked glycosylation modifications for the function of vIL-6 and cellular IL-6, and represents the first example of a differential role of N-glycans in the function of viral and human homologues of the same cytokine. Glycosylated vIL-6 made in eukaryotic cells is at least 1,000 times more potent in stimulating cytokine-dependent cell proliferation than the unglycosylated form of vIL-6 expressed in *E. coli*. vIL-6 made in eukaryotic cells is N-linked glycosylated at two sites, N78 and N89. Based on mutagenesis, only the N89 site is functionally important in engaging the gp130 receptor, JAK/STAT signaling, and stimulation of cell proliferation. The importance of N-linked glycosylation was confirmed by the use of the inhibitor TM, a fungal UDP-GlcNAc–like product that blocks the production of the Glc₃Man₉GlcNAc₂ precursor oligosaccharide required for N-linked glycosylation initiation. In stark contrast, the human cellular homologue, hIL-6, does not require

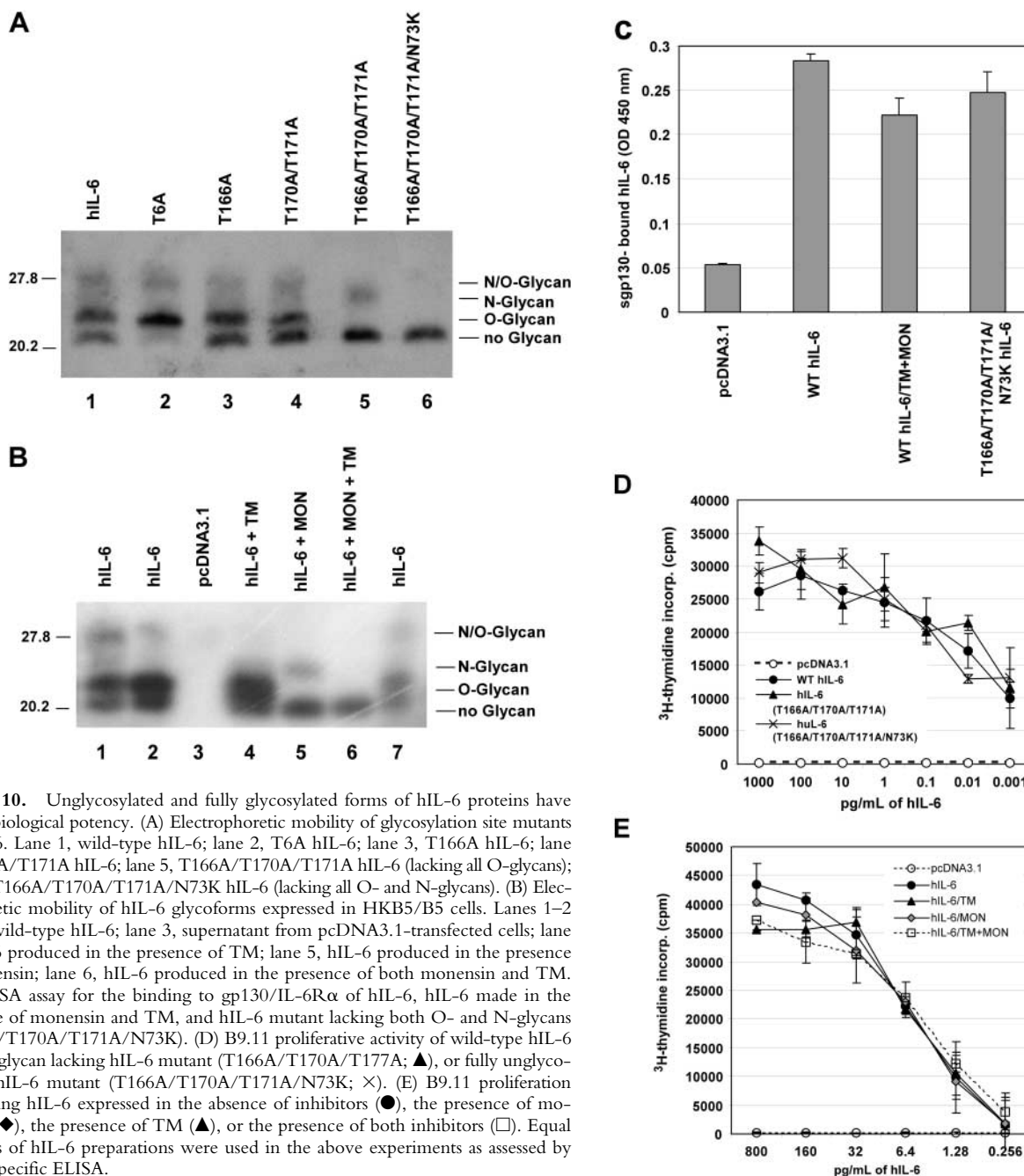


Figure 10. Unglycosylated and fully glycosylated forms of hIL-6 proteins have similar biological potency. (A) Electrophoretic mobility of glycosylation site mutants of hIL-6. Lane 1, wild-type hIL-6; lane 2, T6A hIL-6; lane 3, T166A hIL-6; lane 4, T170A/T171A hIL-6; lane 5, T166A/T170A/T171A hIL-6 (lacking all O-glycans); lane 6, T166A/T170A/T171A/N73K hIL-6 (lacking all O- and N-glycans). (B) Electrophoretic mobility of hIL-6 glycoforms expressed in HKB5/B5 cells. Lanes 1–2 and 7, wild-type hIL-6; lane 3, supernatant from pcDNA3.1-transfected cells; lane 4, hIL-6 produced in the presence of TM; lane 5, hIL-6 produced in the presence of monensin; lane 6, hIL-6 produced in the presence of both monensin and TM. (C) ELISA assay for the binding to gp130/IL-6R α of hIL-6, hIL-6 made in the presence of monensin and TM, and hIL-6 mutant lacking both O- and N-glycans (T166A/T170A/T171A/N73K). (D) B9.11 proliferative activity of wild-type hIL-6 (●), O-glycan lacking hIL-6 mutant (T166A/T170A/T171A) (▲), or fully unglycosylated hIL-6 mutant (T166A/T170A/T171A/N73K) (×). (E) B9.11 proliferation assay using hIL-6 expressed in the absence of inhibitors (●), the presence of monensin (◆), the presence of TM (▲), or the presence of both inhibitors (□). Equal amounts of hIL-6 preparations were used in the above experiments as assessed by hIL-6-specific ELISA.

N-linked glycosylation for optimal function. Mutagenesis of the single site N73 on hIL-6 that is N-linked glycosylated did not affect IL-6R α -dependent gp130 receptor binding, JAK/STAT signaling, or stimulation of B cell proliferation, even with the additional removal of all the O-glycans in hIL-6. These results demonstrate that the KSHV-encoded cytokine not only relies on N-linked glycosylation status for optimal biological function, but also for distinguishing itself from its human homologue.

We also found that the fully glycosylated form of hIL-6 is ~ 100 times more potent in stimulating IL-6-dependent cell proliferation when compared with the fully glycosyl-

ated form of vIL-6. Burger et al. (3) previously reported that equal amounts of unglycosylated hIL-6 was 5,000 times more potent than the vIL-6 counterpart when proteins were made in bacteria. These differences in biological potency when comparing glycosylated and unglycosylated forms of the two IL-6 homologues can be accounted for by our finding that N-linked glycosylation is required for the optimal function of vIL-6, and that vIL-6 expressed in *E. coli* has minimal function. The difference in potency between fully glycosylated forms of hIL-6 and vIL-6 in stimulating cell proliferation might be explained by receptor affinity or the quality of downstream signaling events.

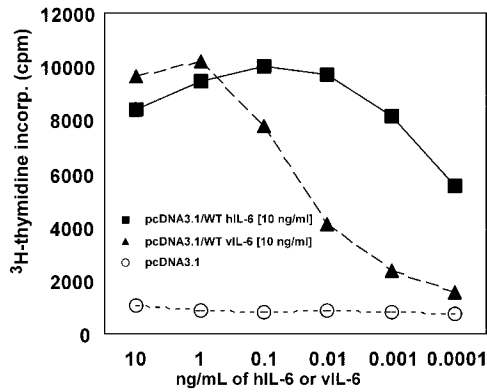


Figure 11. Fully glycosylated hIL-6 is more potent than the KSHV IL-6 counterpart. 10-fold serially diluted supernatants from HKB5/B5 cells transfected with plasmids encoding wild-type hIL-6 or vIL-6, all starting at 10 ng/ml, were assessed for their capacity to stimulate proliferation of B9.11 cells.

Examples of Functional Importance of N-linked Glycosylation of Other Secreted Cellular Cytokines and Growth Factors. Although this report appears to be the first to demonstrate the difference of N-linked glycosylation of closely related viral and cellular cytokine homologues, several examples illustrate the importance of N-linked sugar modifications on the function of cellular-secreted factors. Glycosylation can affect protein stability, specific receptor interaction, and biological activity. For instance, N-linked sugars on human IL-5 have been shown to be important for its thermostability when the protein was incubated at 70°C for 30 min. The de-N-glycosylated hIL-5 was less biologically active after heating (23). Two forms of recombinant IFN-β are currently used as treatment for multiple sclerosis. The fully N-glycosylated form (IFN-β-1a) is at least 10 times more biologically active than the nonglycosylated form (IFN-β-1b). This difference has been attributed to the stabilizing effect of the carbohydrate on the protein structure (24). Recombinant G-CSF is also clinically available in two different forms: lenograstim, the glycosylated form, is more active at increasing absolute neutrophil count in vivo than filgrastim, the deglycosylated form, an effect also attributable to better protein stability (25). Another example is human erythropoietin, a heavily glycosylated protein with multiple glycoforms. Although N-deglycosylated erythropoietin exhibits full biological activity and potency in vitro, its activity in vivo that involves anchoring terminal sialic acids is significantly decreased (26).

Hypotheses to Account for the Functional Importance of N-linked Glycosylation in vIL6. We have considered two hypotheses to account for the essential role of glycosylation of N89. First, N-linked glycosylation of vIL-6 might be required for optimal binding to gp130, either via sugar-sugar or sugar-protein interactions. Gp130 is heavily glycosylated at 9 of the 11 potential N-linked sites (27). Thus, there is ample opportunity for sugar-sugar interaction. A second but not mutually exclusive explanation is the requirement

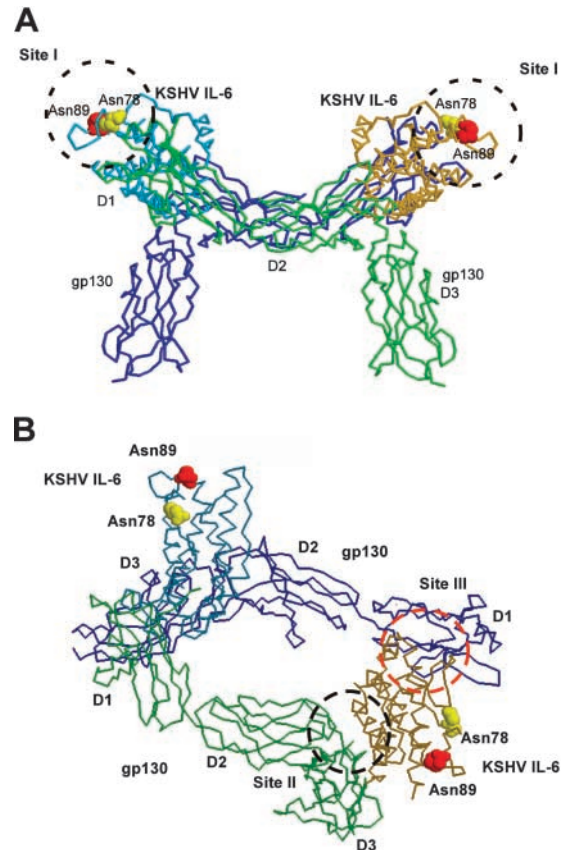


Figure 12. Location of the N-linked glycosylation sites of KSHV-encoded IL-6 on the schematic representation of the cocystal structure of vIL-6 and gp130. Carbon backbone model of vIL-6 and soluble gp130 is shown as a tetrameric complex based on previous crystal structure work, shown in side (A) and tilted view (B; reference 11). A shows site I of vIL-6, which is not a contact site with gp130, but corresponds to a site where hIL-6 interacts with IL6-Rα. B shows one vIL-6 site II (black dotted circle) in contact with D2D3 sites of gp130 molecule (green), and vIL-6 site III (red dotted circle) in contact with D1 site of a second gp130 molecule (blue). N78 (yellow) and N89 (red) are highlighted as space-filling residues and are shown to occupy site I, but not sites II or III. The figure was prepared using the RasMol program (v2.7.1).

of N-linked sugars in N89 for proper folding of vIL-6 into a conformation optimal for interaction with gp130.

The crystal structure of vIL-6 in a complex with the gp130 receptor has been solved (11) and may help to distinguish these alternatives. To achieve the 2.4 Å X-ray cocystal structure resolution, it was necessary to use nonglycosylated forms of the vIL-6 and gp130 proteins produced in insect cells in the presence of the inhibitor TM. Therefore, N-linked glycosylation is not absolutely required for vIL-6 and gp130 interaction. The complex assumes a tetrameric arrangement comprising two vIL-6 proteins and two human gp130 receptors. Each vIL-6 contacts two different gp130 molecules and each gp130 interacts with two vIL-6 molecules, all through structurally distinct binding surfaces (Fig. 12; reference 11). Residues in vIL-6 designated site II interact with domains 2 and 3 (D2D3) of gp130 comprising a cytokine-binding homology region. A second vIL-6 region designated site III interacts with the

NH₂-terminal D1 Ig-like activation domain of a second gp130 molecule. These interactions are required for assembly of a higher order activation complex important for signal transduction (28, 29). It is important to note that the two N-linked glycosylation sites of vIL-6 are located close to each other, but are outside of sites II and III important for cytokine-gp130 receptor interaction (Fig. 12).

vIL-6 has an unused site I facet not occupied by gp130. The equivalent site in hIL-6 interacts with the IL-6R α . N78 and N89 are located in the vicinity of site I. The interaction of IL-6R α with site I of hIL-6 is thought to alter the conformation of cellular cytokine to enable it to bind to gp130 (13, 28). It is notable that N78 and N89 of vIL-6 are located in the vicinity of site I. Therefore, N-linked glycosylation of N89 may substitute for an interaction with IL-R α and change the conformation of the viral cytokine so that it binds gp130. In support of this idea, monoclonal antibodies directed against the epitope D81 to C93 imbedded in the hypothetical site I of vIL-6 and located outside the cytokine-gp130 interface neutralize the viral cytokine by interfering with vIL-6 interaction with gp130 (30). These monoclonal antibodies were postulated to induce conformation changes in vIL-6 that abrogated its function. Our results, taken together with the crystal structure and the effect of neutralizing antibodies, are most consistent with the hypothesis that the N-linked sugars on N89 are critical to establishing the proper conformation of vIL-6 needed to interact with gp130. A potentially important biological consequence of N-linked glycosylation of vIL-6 might be to extend its tropism to cells that contain gp130 and lack IL-6R α . For instance, although both B cells and endothelial cells can be infected by KSHV, only B cells and not endothelial cells express IL-6R α . Further work is needed to characterize the nature of the N-linked sugar side chains and to study the mechanism by which they influence vIL-6 folding.

We gratefully acknowledge Dr. K.C. Garcia (Stanford University, CA) for providing the structure data files, Dr. X.Y. Fu (Yale University, CT) for providing the pGAS/Luc and pLuc reporters, Dr. J. Elias (Yale University, CT) for providing the B9.11 cells, and Dr. A. Iwasaki (Yale University, CT) for helpful discussions.

This work was supported by National Institutes of Health grant CA70036 to G. Miller.

Submitted: 18 July 2003

Accepted: 2 December 2003

References

- Nicholas, J., V.R. Ruvolo, W.H. Burns, G. Sandford, X. Wan, D. Ciuffo, S.B. Hendrickson, H.G. Guo, G.S. Hayward, and M.S. Reitz. 1997. Kaposi's sarcoma-associated human herpesvirus-8 encodes homologues of macrophage inflammatory protein-1 and interleukin-6. *Nat. Med.* 3:287-292.
- Moore, P.S., C. Boshoff, R.A. Weiss, and Y. Chang. 1996. Molecular mimicry of human cytokine and cytokine response pathway genes by KSHV. *Science*. 274:1739-1744.
- Burger, R., F. Neipel, B. Fleckenstein, R. Savino, G. Ciliberto, J.R. Kalden, and M. Gramatzki. 1998. Human herpesvirus type 8 interleukin-6 homologue is functionally active on human myeloma cells. *Blood*. 91:1858-1863.
- Molden, J., Y. Chang, Y. You, P.S. Moore, and M.A. Goldsmith. 1997. Kaposi's sarcoma-associated herpesvirus-encoded cytokine homolog (vIL-6) activates signaling through the shared gp130 receptor subunit. *J. Biol. Chem.* 272:19625-19631.
- Akira, S., T. Taga, and T. Kishimoto. 1993. Interleukin-6 in biology and medicine. *Adv. Immunol.* 54:1-78.
- Kishimoto, T., S. Akira, M. Narazaki, and T. Taga. 1995. Interleukin-6 family of cytokines and gp130. *Blood*. 86:1243-1254.
- Hoischen, S.H., P. Vollmer, P. Marz, S. Ozbek, K.S. Gotze, C. Peschel, T. Jostock, T. Geib, J. Mullberg, S. Mechttersheimer, et al. 2000. Human herpes virus 8 interleukin-6 homologue triggers gp130 on neuronal and hematopoietic cells. *Eur. J. Biochem.* 267:3604-3612.
- Jones, K.D., Y. Aoki, Y. Chang, P.S. Moore, R. Yarchoan, and G. Tosato. 1999. Involvement of interleukin-10 (IL-10) and viral IL-6 in the spontaneous growth of Kaposi's sarcoma herpesvirus-associated infected primary effusion lymphoma cells. *Blood*. 94:2871-2879.
- Aoki, Y., G. Tosato, Y. Nambu, A. Iwamoto, and R. Yarchoan. 2000. Detection of vascular endothelial growth factor in AIDS-related primary effusion lymphomas. *Blood*. 95:1109-1110.
- Somers, W., M. Stahl, and J.S. Seehra. 1997. 1.9 A crystal structure of IL6: implications for a novel mode of receptor dimerization and signaling. *EMBO J.* 16:989-997.
- Chow, D.-C., X.-L. He, A.L. Snow, S. Rose-John, and K.C. Garcia. 2001. Structure of an extracellular gp130 cytokine receptor signaling complex. *Science*. 291:2150-2155.
- Simpson, R.J., A. Hammacher, D.K. Smith, J.M. Matthews, and L.D. Ward. 1997. Interleukin-6: structure-function relationships. *Protein Sci.* 6:929-955.
- Taga, T., and T. Kishimoto. 1997. Gp130 and the interleukin-6 family of cytokines. *Annu. Rev. Immunol.* 15:797-819.
- Chatterjee, M., J. Osborne, G. Bestetti, Y. Chang, and P.S. Moore. 2002. Viral IL-6-induced cell proliferation and immune evasion of interferon activity. *Science*. 298:1432-1435.
- Opdenakker, G., P.M. Rudd, M. Wormald, R.A. Dwek, and J. Van Damme. 1995. Cells regulate the activities of cytokines by glycosylation. *FASEB J.* 9:453-457.
- Orita, T., M. Oh-eda, M. Hasegawa, H. Kuboniwa, K. Esaki, and N. Ochi. 1994. Polypeptide and carbohydrate structure of recombinant human interleukin-6 produced in Chinese hamster ovary cells. *J. Biochem.* 115:345-350.
- El-Guindy, A.S., L. Heston, Y. Endo, M.S. Cho, and G. Miller. 2002. Disruption of Epstein-Barr virus latency in the absence of phosphorylation of ZEBRA by protein kinase C. *J. Virol.* 76:11199-11208.
- Jablons, D.M., J.J. Mule, J.K. McIntosh, P.B. Sehgal, L.T. May, C.M. Huang, S.A. Rosenberg, and M.T. Lotze. 1989. IL-6/IFN-beta-2 as a circulating hormone. Induction by cytokine administration in humans. *J. Immunol.* 142:1542-1547.
- Bock, G.H., C.A. Long, M.L. Riley, J.D. White, C.C. Kurman, T.A. Fleisher, M. Tsokos, M. Brown, D. Serbousek, W.D. Schwietermann, et al. 1993. Characterization of a new IL-6-dependent human B-lymphoma cell line in long term culture. *Cytokine*. 5:480-489.
- Sun, R., S.F. Lin, K. Staskus, L. Gradoville, E. Grogan, A. Haase, and G. Miller. 1999. Kinetics of Kaposi's sarcoma-associated herpesvirus gene expression. *J. Virol.* 73:2232-2242.
- Wan, X., H. Wang, and J. Nicholas. 1999. Human herpesvirus 8 interleukin-6 (vIL-6) signals through gp130 but has

- structural and receptor-binding properties distinct from those of human IL-6. *J. Virol.* 73:8268–8278.
22. Osborne, J., P.S. Moore, and Y. Chang. 1999. KSHV-encoded viral IL-6 activates multiple human IL-6 signaling pathways. *Hum. Immunol.* 60:921–927.
 23. Kodama, S., M. Tsujimoto, N. Tsuruoka, T. Sugo, T. Endo, and A. Kobata. 1993. Role of sugar chains in the in vitro activity of recombinant human interleukin-5. *Eur. J. Biochem.* 211:903–908.
 24. Runkel, L., W. Meier, R.B. Pepinsky, M. Karpusas, A. Whitty, K. Kinball, M. Brickelmaier, C. Muldowney, W. Jones, and S.E. Croelz. 1998. Structural and functional differences between glycosylated and non-glycosylated forms of human interferon- β (IFN- β). *Pharm. Res.* 15:641–649.
 25. Nohynek, G.J., J.P. Plard, M.Y. Wells, A. Zerial, and F. Roquet. 1996. Comparison of the potency of glycosylated and nonglycosylated recombinant human granulocyte colony-stimulating factors in neutropenic and nonneutropenic CD rats. *Cancer Chemother. Pharmacol.* 39:259–266.
 26. Higuchi, M., M. Oh-Eda, H. Kuboniva, K. Tomonoh, Y. Shimanoka, and N. Ochi. 1992. Role of sugar chains in the expression of the biological activity of human erythropoietin. *J. Biol. Chem.* 267:7703–7709.
 27. Moritz, R.L., N.E. Hall, L.M. Connolly, and R.J. Simpson. 2001. Determination of the disulfide structure and N-glycosylation sites of the extracellular domain of the human signal transducer gp130. *J. Biol. Chem.* 276:8244–8253.
 28. Chow, D.C., L. Brevnova, X.L. He, M.M. Martick, A. Bankovich, and K.C. Garcia. 2002. A structural template for gp130-cytokine signaling assemblies. *Biochim. Biophys. Acta.* 1592:225–235.
 29. Chow, D., J. Ho, T.L. Nguyen Pham, S. Rose-John, and K.C. Garcia. 2001. In vitro reconstitution of recognition and activation complexes between interleukin-6 and gp130. *Biochemistry.* 40:7593–7603.
 30. Aoki, Y., M. Narazaki, T. Kishimoto, and G. Tosato. 2001. Receptor engagement by viral interleukin-6 encoded by Kaposi sarcoma-associated herpesvirus. *Blood.* 98:3042–3049.